

Nonisothermal Crystallization Kinetics of Poly(ethylene terephthalate) and Poly(methyl methacrylate) Blends

Ahmed Bishara, Habib I. Shaban

Chemical Engineering Department, Kuwait University, P.O. Box 5969, 13060 Safat, Kuwait

Received 2 December 2004; accepted 7 April 2005

DOI 10.1002/app.22440

Published online in Wiley InterScience (www.interscience.wiley.com).

ABSTRACT: The nonisothermal crystallization kinetics of poly(ethylene terephthalate) (PET) and poly(methyl methacrylate) (PMMA) blends were studied. Four compositions of the blends [PET 25/PMMA 75, PET 50/PMMA 50, PET 75/PMMA 25, and PET 90/PMMA 10 (w/w)] were melt-blended for 1 h in a batch reactor at 275°C. Crystallization peaks of virgin PET and the four blends were obtained at cooling rates of 1°C, 2.5°C, 5°C, 10°C, 20°C, and 30°C/min, using a differential scanning calorimeter (DSC). A modified Avrami equation was used to analyze the nonisothermal data obtained. The Avrami parameters n , which denotes the

nature of the crystal growth, and Z_t , which represents the rate of crystallization, were evaluated for the four blends. The crystallization half-life ($t_{1/2}$) and maximum crystallization (t_{max}) times also were evaluated. The four blends and virgin polymers were characterized using a thermogravimetric analyzer (TGA), a wide-angle X-ray diffraction unit (WAXD), and a scanning electron microscope (SEM). © 2006 Wiley Periodicals, Inc. *J Appl Polym Sci* 101: 3565–3571, 2006

Key words: nonisothermal crystallization; PET–PMMA blends; crystallization kinetics

INTRODUCTION

The commercial development of polymer blends has been immensely important in recent years because production of the blends are more favorable economically compared to the more conventional chemical routes for making new products. Blend systems, which are composed of existing materials, can be developed at reduced cost in order to suit new market requirements.¹ Because the properties of a blend system vary with the composition, an existing blend can be easily and quickly modified to meet performance and cost objectives required for new or changing markets. Discounting research and development costs, new blend systems are particularly attractive when one of the components is much less expensive than the others because this allows the blend to be produced at a low cost.^{2–4} Blends also can be commercially rewarding if they improve processability and performance.

Polymer blending is an attractive alternative for producing new polymeric materials with desirable properties without having to synthesize a totally new material. Other advantages of polymer blending are versatility, simplicity, and inexpensiveness. There have been numerous articles in the literature on various aspects of binary blends of polyesters, including

blends of PET, PBT,^{5–12} poly(trimethylene terephthalate) (PTT), and polyetherimide (PEI).¹³

Escala and Stein⁵ reported that PET/PTT blends showed a single, composition-dependent glass-transition temperature (T_g) at all compositions, suggesting that PET and PTT were miscible in the amorphous state. Similar results were reported by others.^{9–10}

Recently, Huang and Chang¹³ investigated the miscibility, melting, and crystallization behavior of PTT/PEI blends. They observed that the blends exhibited a single, composition-dependent T_g over the entire composition range studied, indicating that the blends were fully miscible in the amorphous state.

Research on blends containing more than two components promises more sophisticated commercial blends in the future.

The material properties for engineering thermoplastic applications are a high heat distortion temperature (HDT), toughness, solvent resistance, low cost, and ease of molding, which usually means a highly shear-dependent melt viscosity at moderate temperature, combined with good melt thermal stability. No material, blend, or homopolymer meets all these criteria. High-melting polyesters and polyamides meet most of the requirements, although mold shrinkage and mechanical properties depend on the crystallization rate.

Continued growth in new polymer blends is expected, driven by the need to combine high-performance characteristics such as strength and toughness with resistance to heat and aggressive chemical environments.

The miscibility of polymer blends has been investigated extensively, both theoretically and experimen-

Correspondence to: Habib I. Shaban (maths@kuc01.kuniv.edu.kw)

Contract grant sponsor: Kuwait University; contract grant number: EC 01/02.

tally, in the past few decades. The nature and characteristics of amorphous/amorphous and amorphous/crystalline polymer blends are well accepted.^{14,15}

Studies related to the kinetics of polymer crystallization are of great importance in polymer processing because the resulting physical properties are strongly dependent on the morphology formed and the extent of crystallization during processing. It therefore is very important to understand the processing–structure–property interrelationships of the materials studied.

The crystallization behavior of PET and its blends is important for the manufacture of plastics because the physical properties of the blends depend on the crystallinity, morphology, and glass-transition temperature. Crystal structure and morphology (crystallization conditions) are responsible for the properties of the final product. A sound knowledge and understanding of crystallization mechanisms are necessary for being able to designing materials with better mechanical properties.

In the present work the nonisothermal crystallization kinetics of blends of PET and PMMA, was compared to those of virgin PET and virgin PMMA using a differential scanning calorimeter (DSC). The nonisothermal crystallization kinetic parameters such as the modified Avrami constant (n), the crystallization growth rate (Z_i), and the half-life ($t_{1/2}^i$) and maximum crystallization (t_{max}) times were determined.

The virgin polymers and the blends were characterized using thermogravimetric analysis to determine weight loss. Wide-angle X-ray diffraction was used to determine the crystalline content of the virgin polymers and the blends. Scanning electron microscopy was used to study the morphology of the virgin PET, the virgin PMMA, and the blends.

The objectives in this work were: (1) to assess the miscibility of the blends, (2) to investigate the effect of blend composition on nonisothermal melt crystallization, and (3) to assess the effect of blend composition on degree of crystallinity.

EXPERIMENTAL

Materials

Bottle-grade PET in pellet form was obtained from Century Enka Pvt. Ltd. (India). The intrinsic viscosity of the resin was 0.60 g/dL, measured at 28°C with a Cannon Ubbelohde viscometer. Virgin PMMA was used that had been injection-molded in sheet form at an injection pressure of 10,000–15,000 psi, a cylinder temperature of 177°C–210°C, and a mold temperature of 79°C–107°C. The molded PMMA sheet had a specific gravity of 1.18, tensile strength of 9000 psi, flexural strength of 15,000 psi, and an intrinsic viscosity of 0.64 g/dL.

Sample preparation

Four compositions of PET and PMMA (25 : 75, 50 : 50, 75 : 25, and 90 : 10) resins (weight basis) were dried in a vacuum oven at 100°C for 5 h. The polymers were melt-mixed in a reactor at a stirrer speed of 100 rpm for 1 h at 275°C. The blended product was then removed from the reactor and ground using a domestic mixer grinder.

Nonisothermal crystallization studies

A Mettler-Toledo TA 4000 differential scanning calorimeter was used to record the nonisothermal melt-crystallization exotherms for virgin PET and the PET/PMMA blends. Calibration of the temperature scale was carried out with a pure indium standard ($T_m = 156.6^\circ\text{C}$ and $\Delta H_f = 28.5 \text{ J/g}$) to ensure the accuracy and reliability of the data obtained. Temperature calibration of the DSC instrument was carried out using a standard pan consisting of three metals, indium, lead, and zinc, whose melting temperatures were 156.6°C, 327.4°C, and 419.5°C, respectively. These temperatures were automatically recorded in the instrument after calibration. Each sample was used only once, and all the runs were carried out under a nitrogen atmosphere in order to prevent extensive thermal degradation.

For the DSC experiments, PET, PMMA, and the blends were heated from 30°C to 280°C at a rate of 10°C/min under a nitrogen atmosphere. A melt annealing time of 10 min was maintained at 280°C for all samples, which were then cooled to 30°C at a cooling rate of 10°C/min. The crystallization enthalpy (j/g) and peak melting temperature of crystallization (P_k°)C for both the heating and cooling cycles were calculated.

Nonisothermal studies of the blends and virgin polymers were carried out at cooling rates per minute of 1°C, 2.5°C, 5°C, 10°C, 20°C, and 30°C from 280°C to 175°C.

For a typical run, the sample was heated in the DSC furnace from 30°C to 280°C at a heating rate of 10°C/min under a nitrogen atmosphere. After a melt annealing period of 10 min at 280°C the sample was cooled to 175°C at 1°C/min. The sample was then cooled to 30°C at a rate of 100°C/min.

Polymer characterization

TGA analysis

The decomposition temperatures for PET, PMMA, and the blends were measured using an SDT 2960 simultaneous DSC-TGA instrument supplied by TA Instruments Ltd. The heating rate was 20°C/min, and the temperature range scanned went from 30°C to 650°C. Then weight loss of the virgin polymers and the blends was determined.

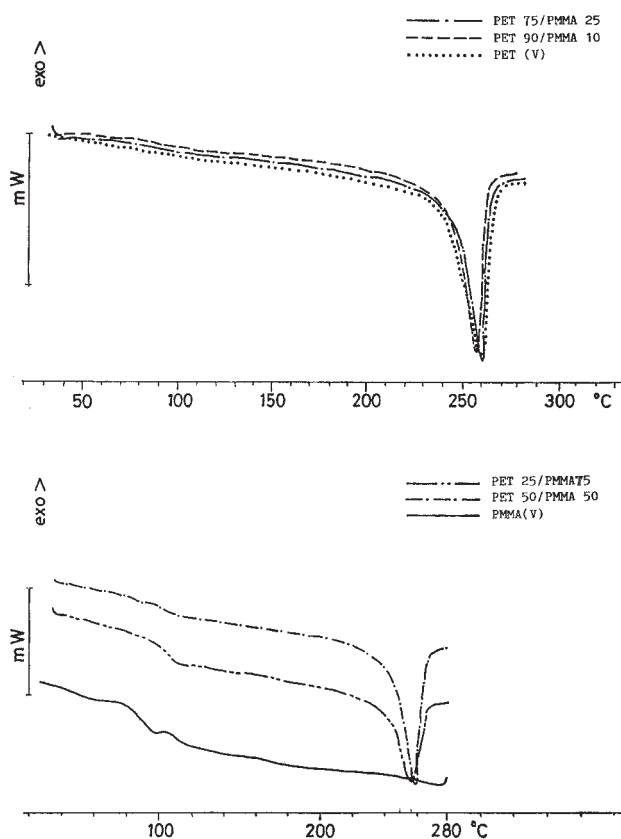


Figure 1 Heating curves for virgin PET, virgin PMMA and blends of PET/PMMA

Wide-angle X-ray diffraction

The X-ray diffractometry (XRD) technique was used to determine the crystal modification and the apparent degree of crystallinity of the PET, PMMA, and blended samples. XRD measurement was carried out with a Siemens D 5000 X-ray powder diffractometer that had computerized data collection and an analytical tool box. The wavelength (λ) of the Cu tube was 1.5406 Å*. The theta start position was 10°, and the stop position was 80°. The X-ray source (Cu α radiation, $\lambda = 1.54$ Å*) was generated with an applied voltage of 40 kV and a filament current of 30 mA*.

Scanning electron microscopy

Scanning electron microscopy (SEM) with a Joel model 6300 was used to check the morphology of the virgin materials and the blends. The microscope had an exL II energy dispersive spectroscope. The samples were coated with a thin layer of gold prior to SEM observation. SEM analysis was carried out at magnifications of 350 and 1500.

RESULTS AND DISCUSSION

The nonisothermal crystallization kinetics of virgin PET and the PET/PMMA blends were studied using a

Mettler DSC 30 unit. The heating curves for virgin PET, virgin PMMA, PET 25/PMMA 75, PET 50/PMMA 50, PET 75/PMMA 25, and PET 90/PMMA 10 were obtained at 10°C/min are shown in Figure 1. A glass-transition temperature (T_g) of 90°C was noted for the PMMA. The PET was heated at 10°C/min from room temperature to 280°C and then quench-cooled. Then in a second cycle, it was reheated to 280°C again at 10°C/min. No T_g was noted in the second cycle. This could have been a result of the material characteristic of the chosen PET. For the PET 25/PMMA 75 and PET 50/PMMA 50 blends, a T_g of around 105°C was noted, whereas for PET 75/PMMA 25 and PET 90/PMMA 10, no T_g was noted. The T_g noted for the PET 25/PMMA 75 and PET 50/PMMA 50 blends could be that of PMMA, which had shifted slightly to 105°C. The shift could have been a result of there being more PMMA. The melting peaks of all the polymers except PMMA were between 255°C and 260°C, as can be seen in Figure 1. Also observed was that as the PET content increased, the enthalpy value, ΔH , increased (Table I).

Figure 2 shows typical exotherms for PET 25/PMMA 75 obtained at different cooling rates. The exotherms were found to broaden with an increasing cooling rate. The enthalpy values of the exotherms were found to decrease as the cooling rate increased

TABLE I
Enthalpy Values and Peak Melting Temperatures

Composition of the PET/PMMA Blend	T_m^* (°C)	ΔH (J/gm)	P_k (°C)
PET 25/PMMA 75	218	5.8	253.8
	219.5	6.0	248.7
	222	6.2	249.8
	223	6.5	250.5
PET 50/PMMA 50	211	19.3	254
	217.3	16.5	252.1
	219.5	15.8	250
	222.2	16.8	250.6
	224.2	17.5	251
PET 75/PMMA 25	207	31.4	254.5
	217	28.4	254
	220	25.9	250
	223	27.7	250.6
	226	28.2	251.8
PET 90/PMMA 10	198	25.5	254.1
	207	31.2	253.9
	211	31.3	254.0
	215	32.1	253.3
	221	33.1	250.5
Virgin PET		37.1	255.5

T_m^* Typical temperatures from first cooling cycle fixed for obtaining nonisothermal enthalpy values at a cooling rate of 10°C/min.

ΔH , Enthalpy value of melting (J/gm) in the first heating cycle for the corresponding selected temperature (rate is 10°C/min).

P_k , Peak melting temperature (°C) obtained in the first heating cycle.

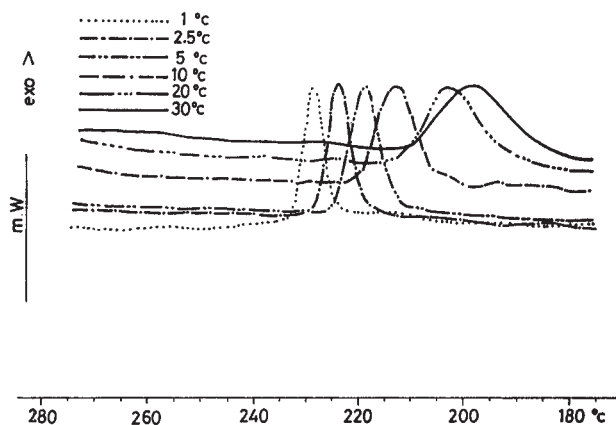


Figure 2 Non isothermal curves for PET 25/PMMA 75

(Table II). A similar trend was noted for the cooling peak temperature (P_k). Similar findings were observed for PET 50/PMMA 50, PET 75/PMMA 25, PET 90/PMMA 10, and virgin PET, indicating that at the maximum cooling rate, crystallization shifted to a lower temperature.

From the DSC plots a relationship between nonisothermal crystallization temperature (T) and time (t)¹⁶ can be given as:

$$t = \frac{[T_0 - T]}{\phi} \quad (1)$$

where T_0 is the initial temperature at which crystallization begins at zero time and ϕ is the cooling rate.

Figure 3 shows a typical plot of relative crystallinity, $X(t)$, as a function of temperature, T , for PET 25/

TABLE II
Nonisothermal Crystallization Parameters of PET-Virgin and the Four Blends

ϕ (°C/min)	P_k (°C)	ΔH (J/gm)	n	Z_t	$t_{1/2}$ (min)	t_{\max} (min)
PET 25/PMMA 75						
1	229	14.8	1.4	4.39	0.26	0.14
2.5	224.3	10.9	1.6	2.45	0.45	0.30
5	219.6	12.2	1.8	2.01	0.55	0.43
10	213.6	10.2	3.3	1.64	0.76	0.77
20	206.6	10.4	3	1.04	0.87	0.86
30	200.8	9.2	4	1.65	0.80	0.82
PET 50/PMMA 50						
1	230.3	26.4	1	2.32	0.29	0.02
2.5	225.8	27.4	1.3	1.95	0.44	0.19
5	221.8	26.2	1.1	1.24	0.58	0.09
10	216.4	27.1	1.5	1.29	0.66	0.40
20	208.7	25.4	2.4	1.18	0.80	0.74
30	204.1	21.8	3.6	1.73	0.77	0.78
PET 75/PMMA 25						
1	232.1	42.7	1.2	2.86	0.30	0.09
2.5	228.2	41.5	1.1	1.70	0.44	0.06
5	226	45.3	1	1.03	0.67	0.07
10	220.4	38	2.1	1.03	0.82	0.72
20	215.1	38.1	2.3	1.31	0.75	0.69
30	211.1	38.3	2.4	1.56	0.71	0.06
PET 90/PMMA 10						
1	227.7	46.6	2.2	10.40	0.29	0.26
2.5	223.5	43.3	1.7	2.74	0.44	0.32
5	222.2	22.9	2.6	2.07	0.65	0.62
10	216.4	27.9	1.9	1.14	0.76	0.62
20	210	24.2	2.5	1.27	0.78	0.73
30	200.5	28.5	5	1.91	0.81	0.84
PET-Virgin						
1	225.1	48.3	2.21	10.54	0.29	0.26
2.5	220.7	44.1	1.78	3.08	0.43	0.33
5	219.2	31.3	1.87	2.00	0.56	0.45
10	214.2	23.4	1.78	1.19	0.73	0.56
20	207.3	16.2	2.54	1.28	0.78	0.74
30	195.1	25.1	5	1.91	0.81	0.83

ϕ , Cooling rate (°C/min).

P_k , Peak crystallization temperature (°C).

ΔH , Enthalpy value for crystallization (J/gm).

n , Avrami constant.

Z_t , Crystallization rate constant.

$t_{1/2}$, Crystallization half-life (min).

t_{\max} , Maximum crystallization time (min).

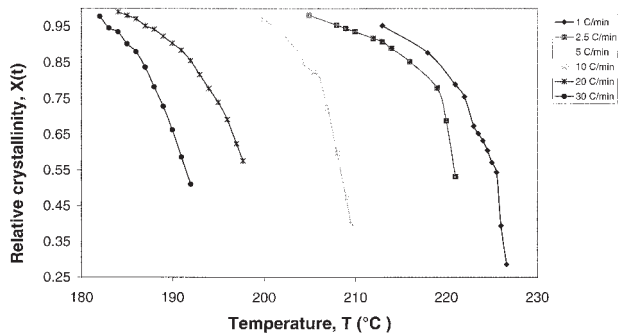


Figure 3 Plot of relative crystallinity $X(t)$ at different crystallization temperatures T ($^{\circ}\text{C}$) for PET25/PMMA75.

PMMA 75. As can be seen in Figure 3, as the cooling rate increased, crystallization occurred at a lower temperature. Also noted was that the relative crystallinity for a particular cooling rate was at a lower temperature, which decreased as the temperature rose.

Figure 4 shows a typical plot of relative crystallinity, $X(t)$, as a function of crystallization time, t , in minutes, for PET 25/PMMA 75. The data for these plots were obtained from eq. (1). Figure 4 also shows a curved pattern for the cooling rates per minute of 1°C , 2.5°C , 5°C , and 10°C and almost a straight line for the cooling rates of $20^{\circ}\text{C}/\text{min}$ and $30^{\circ}\text{C}/\text{min}$.

Mandelkern et al.¹⁶ modified the Avrami equation and reported the following equations for the determination of the crystallization parameters:

$$1 - X(t) = \exp[-Z_t t^n] \quad (2)$$

$$\log\{-\ln[1 - X(t)]\} = n \log t + \log Z_t \quad (3)$$

where Z_t is the nonisothermal crystallization rate constant, and $X(t)$ is the relative crystallinity. A typical plot using eq. (3) for the nonisothermal crystallization process at different cooling rates is shown in Figure 5. The values of n and Z_t , which were obtained using the modified Avrami equation, are given in Table II. Jezi-

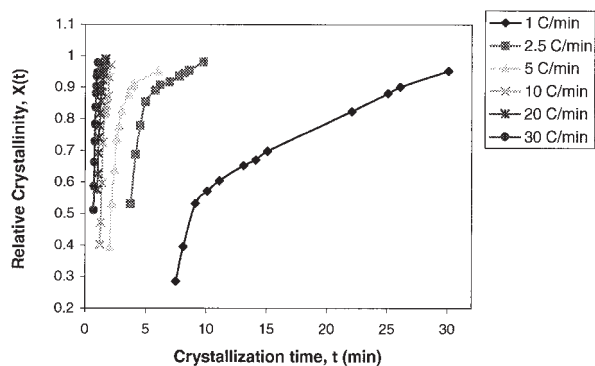


Figure 4 Relative crystallinity $X(t)$ at different crystallization times (t) for non-isothermal crystallization of PET25/PMMA75.

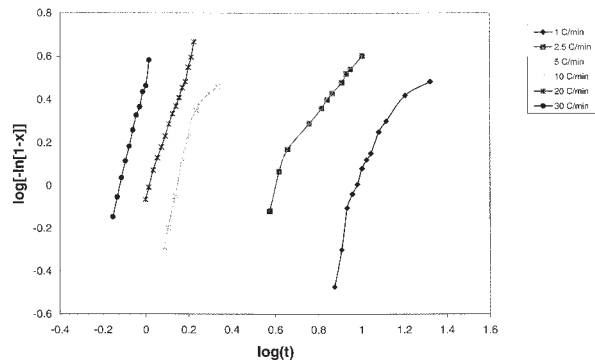


Figure 5 Plot of $\log\{-\ln[1 - X(t)]\}$ versus $\log(t)$ for the non-isothermal crystallization of PET25/PMMA75.

orney¹⁷ considered the crystallization process to consist of two stages: (1) the primary stage, when the value of the crystallization rate constant (n) lies between 1 and 5, and (2) the secondary stage, when the crystallization rate constant is above 5. The Avrami parameter (n), which indicates crystal size, was found to increase as a function of the crystallization rate. The values of n were in the range of 1–5 at different cooling rates (ϕ), indicating that only primary-stage crystallization occurred for the blends under study.

The rate constant, Z_t , was found to decrease as a function of cooling rate for all blend compositions. Z_t varied between 10.5 and 1. The values of n and Z_t were obtained using the linear trendline program of Excel 2000.

The crystallization half-time, $t_{1/2}^1$, was defined as the time at which 50% of the crystallization had been completed 50%. It was determined from the measured kinetic parameters using the following equation:

$$t_{1/2}^1 = \left(\frac{\ln 2}{Z_t}\right) \quad (4)$$

The $t_{1/2}^1$ values obtained from eq. (4) are given in Table II. The $t_{1/2}^1$ was found to increase as a function of the cooling rate, and it varied from 0.26 to 0.87 min. Figure

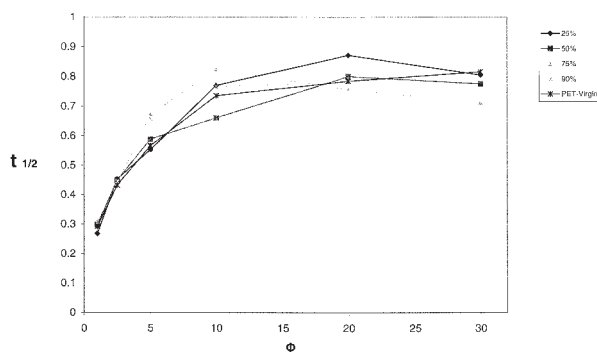


Figure 6 Plot indicating variation of $t_{1/2}^1$ as a function of cooling rate (ϕ) for PET-virgin and PET/PMMA blends.

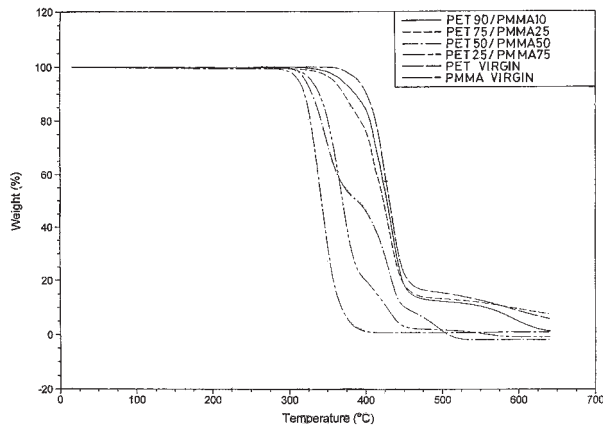


Figure 7 TGA curves for virgin PET, virgin PMMA and PET/PMMA blends

6 shows the variation in $t_{\frac{1}{2}}$ as a function of the cooling rate. It can be seen from Figure 6 that the $t_{\frac{1}{2}}$ values increased as a function of the cooling rate (ϕ).

The t_{\max} , the time necessary for maximum crystallization to occur, was calculated using the following equation:

$$t_{\max} = \left(\frac{n-1}{nZ_t} \right)^{1/n} \quad (5)$$

where n and Z_t were obtained from eq. (3). The value of t_{\max} was found to increase as a function of the cooling rate (ϕ), and it varied from 0.02 to 0.86 for virgin PET and the blends.

Polymer characterization

TGA characterization

Figure 7 shows the TGA curves of the virgin materials and the four blends. Figure 7 also indicates that virgin PET had greater thermal stability than did virgin PMMA and that as the PET content of the blend increased, thermal stability increased.

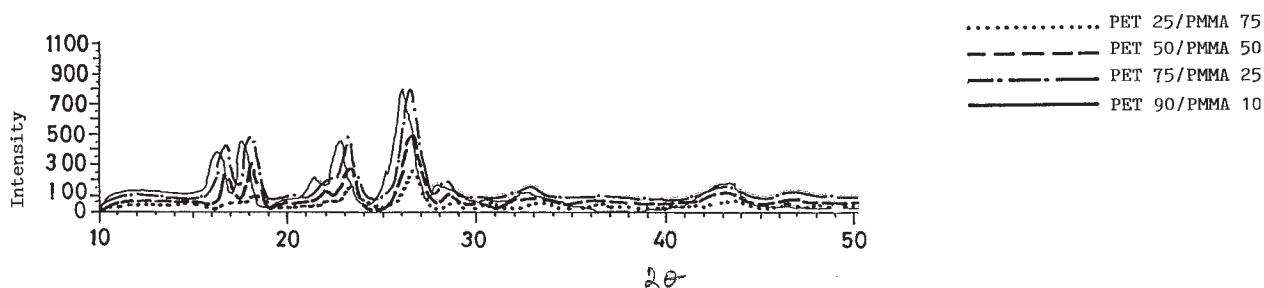


Figure 8 X ray plot for PET/PMMA blends

X-ray analysis

X-ray analysis of the virgin materials (PET, PMMA) and the four blends indicated that PMMA is a glassy material because of the absence of crystalline peaks and that virgin PET is a semicrystalline material because of the presence of crystalline peaks.

Figure 8 shows a typical X-ray plot for PET/PMMA blends. The plot shows that as PET content increased in the blend, the sharpness of the peak and the area under the peak increased, indicating an increase in crystallinity.

Scanning electron microscope (SEM)

Typical scanning electron micrographs of PET 90/PMMA 10 are shown in Figure 9. Two magnifications, 350 and 1500, were obtained for all samples.

Figure 9, a micrograph of the PET 90/PMMA 10 blend, shows blocks of PMMA in the PET base, indicating the immiscible nature of the PET/PMMA blend.

CONCLUSIONS

The study of nonisothermal crystallization kinetics of virgin PET and four PET/PMMA blends was carried out with a differential scanning calorimeter.

Six cooling rates per minute—1°C, 2.5°C, 5°C, 10°C, 20°C, and 30°C—were employed to study nonisothermal crystallization kinetics. The peak crystallization temperatures (P_k) and the enthalpy values (ΔH) at different cooling rates were determined. The P_k and ΔH were found to decrease as a function of the cooling rate. Highest crystallization enthalpy value was found for virgin PET. A modified Avrami equation was used to obtain the crystallization parameters such as the Avrami constant (n) and the crystallization growth rate (Z_t).

The Avrami exponent (n) was found to vary between 1 and 5. The value of n was found to increase as a function of the cooling rate (ϕ). The rate constant (Z_t) was found to decrease with increasing cooling rate for all four compositions. The values of Z_t for PET 90/

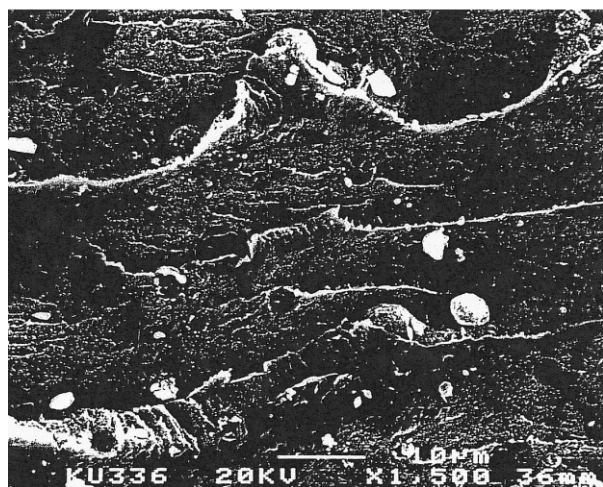
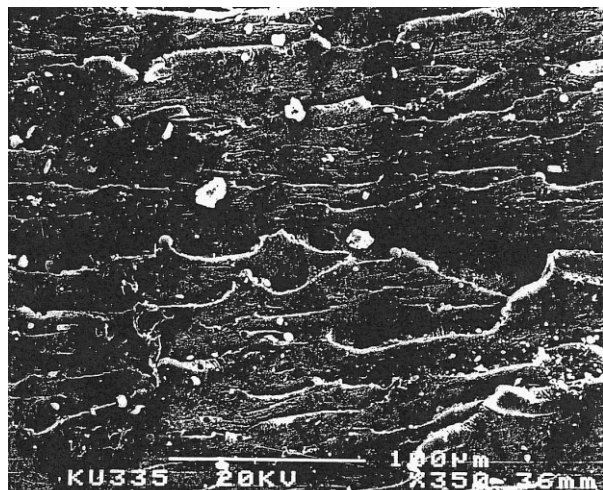


Figure 9 Scanning electron micrograph for PET90/PMMA10

PMMA 10 blend were very close to those of the virgin PET, indicating that the rate of crystallization was almost identical for the PET 90/PMMA 10 blend and virgin PET. The half-life ($t_{1/2}$) and maximum crystallization (t_{max}) times also were evaluated. The values of t_{max} were slightly less than the ($t_{1/2}$) values, indicating that maximum crystallization took place in a shorter time.

The virgin materials and blends were characterized using a thermogravimetric analyzer, a wide-angle X-ray diffraction unit, and a scanning electron microscope.

The TGA curves indicate that virgin PET had greater thermal stability than the virgin PMMA, and as the PET content of the blend increased, the thermal stability increased.

X-ray analysis indicated that PMMA was a glassy material because of the absence of a crystallization peak and that the virgin PET was a semicrystalline material because of the presence. As the PET content increased, the blend area under the peak increased, indicating increased crystallinity.

The SEM micrograph of PET 90/PMMA 10 blends showed blocks of PMMA in the PET base, indicating the immiscible nature of the PET/PMMA blend.

The authors are grateful to Dr. Johnson Mathew and R. Thangakunam, Kuwait University, for their professional help during the course of this work. Mr. Mohammed Rafique, Electron Microscopy Unit, Science Faculty, Kuwait University, for carrying out the scanning electron microscopy analysis and the XRD Section, SAF, for carrying out the XRD analysis.

References

1. Chem Week 72 (Mar. 1, 1983).
2. Robeson, L. M. *Polym Eng Sci* 1984, 24, 587.
3. Utracki, L. A. *Polym Eng Sci* 1982, 22, 1166.
4. Barlow, J. W.; Paul, D. R. *Polym Eng Sci* 1981, 21, 985.
5. Escala, A.; Stein, R. S. *Adv Chem Ser* 1979, 176, 455.
6. Mishra, S. P.; Deopura, B. L. *Polym Commun* 1985, 26, 5.
7. Mishra, S. P.; Deopura, B. L. *J Appl Polym J* 1987, 33, 759.
8. Avramov, I.; Avramov, N.; *J Macromol Sci, Phys* 1991, 30, 335.
9. Shonaike, G. O. *Eur Polym J* 1992, 28, 777.
10. Yu, Y.; Choi, K. *J Polym Eng Sci* 1997, 37, 91.
11. Lee, S. S.; Kim, J.; Park, M.; Lim, S.; Chul, R. C. J. *Polym Part B, Polym Phys* 2001, 39, 22589.
12. Nabi Saheb, D.; Jog, J. P. *Polym Sci Part B, Polym Phys* 1999, 37, 2439.
13. Huang, J. M.; Chang, F. C. *J Appl Polym Sci* 2002, 84, 850.
14. Paul, D. R.; Newman, S., Eds. *Poly Blends*; Academic Press: London, 1978; Vols. I and II.
15. Coleman, M. M.; Graf, J. F.; Painter, P.C. *Specific Interactions and Miscibility of Polymer Blends*; Technomic: Lancaster, PA, 1991.
16. Mandelkern, L.; Fatou, J. G.; Marco, C. *Polymer* 1990, 31, 1685.
17. Jeziorny, A. *Polymer* 1984, 19, 1142.